An Exosuit System With Bidirectional Hand Support for Bilateral Assistance Based on Dynamic Gesture Recognition

Zhichuan Tang, Zhihao Zhu, Shengye Lv, Xuanyu Hong, Yuxin Peng, *Member, IEEE*, and Nuo Chen

***Abstract*— Hand motor impairment has seriously affected the daily life of the elderly. We developed an electromyography (EMG) exosuit system with bidirectional hand support for bilateral coordination assistance based on a dynamic gesture recognition model using graph convolutional network (GCN) and long short-term memory network (LSTM). The system included a hardware subsystem and a software subsystem. The hardware subsystem included an exosuit jacket, a backpack module, an EMG recognition module, and a bidirectional support glove. The software subsystem based on the dynamic gesture recognition model was designed to identify dynamic and static gestures by extracting the spatio-temporal features of the patient's EMG signals and to control glove movement. The offline training experiment built the gesture recognition models for each subject and evaluated the feasibility of the recognition model; the online control experiments verified the effectiveness of the exosuit system. The experimental results showed that the proposed model achieve a gesture recognition rate of 96.42% ± 3.26%, which is higher than the other three traditional recognition models. All subjects successfully completed two daily tasks within a short time and the success rate of bilateral coordination assistance are 88.75% and 86.88%. The exosuit system can effectively help patients by bidirectional hand support strategy for bilateral coordination assistance in daily tasks, and the proposed method can be applied to various limb assistance scenarios.**

Manuscript received 20 May 2024; revised 8 August 2024; accepted 21 August 2024. Date of publication 26 August 2024; date of current version 3 September 2024. This work was supported in part by the Philosophy and Social Science Planning Fund Project of Zhejiang Province under Grant 24ZJQN086Y, in part by the Key Research and Development Program of Zhejiang Province under Grant 2022C03148, and in part by the National Social Science Fund of China under Grant 22CTQ016. *(Corresponding author: Yuxin Peng.)*

This work involved human subjects or animals in its research. Approval of all ethical and experimental procedures and protocols was granted by the Ethics Committee of the Industrial Design Institute, Zhejiang University of Technology, under Application No. 0412/2023/20230012.

Zhichuan Tang is with the Industrial Design Institute, Zhejiang University of Technology, Hangzhou 310023, China, and also with the Modern Industrial Design Institute, Zhejiang University, Hangzhou 310013, China (e-mail: ztang@zjut.edu.cn).

Zhihao Zhu, Shengye Lv, Xuanyu Hong, and Nuo Chen are with the Industrial Design Institute, Zhejiang University of Technology, Hangzhou 310023, China.

Yuxin Peng is with the College of Education, Zhejiang University, Hangzhou 310058, China (e-mail: yxpeng@zju.edu.cn).

Digital Object Identifier 10.1109/TNSRE.2024.3449338

***Index Terms*— Exosuits, electromyography, bilateral assistance, exoskeletons.**

I. Introduction

WITH aging of society, the degeneration of hand function among the elderly leads to serious difficulties in performing activities of daily living (ADL) [1]. Physical therapy is needed for improving hand function [2]. Repetitive task practice (RTP) rehabilitation can improve hand motor performance [3], but it is difficult for patients to complete RTP rehabilitation independently [4]. Therefore, the use of appropriate robotic equipment to assist the elderly becomes important [5].

Exoskeletons have been commonly used for assistance and rehabilitation [6]. Most of them include two main types: rigid exoskeletons and soft exoskeletons. Rigid exoskeletons offer good support and high torque, but they have inherent disadvantages such as being bulky, expensive, and time-consuming to wear [7]. Therefore, soft exoskeleton devices have been proposed as exosuits [8]. Exosuits are lightweight, low-cost and easy to wear due to the use of fabric materials. The flexibility makes exosuits promising for providing better assistance and rehabilitation [9]. Research on exosuits and hand rehabilitation devices is growing. Lessard et al. [10] proposed a portable exosuit (CRUX) that can enhance the wearer's abilities through power-lines. Abe et al. [11] proposed a soft power support suit (18 Weave) that used a thin McKibben muscle to achieve flexibility and adaptability. Bernardo et al. [12] designed an exosuit that combined an elbow exosuit and a hand exoskeleton. Leonardis et al. [13] proposed a hand exoskeleton (BRAVO), which was driven by electromyography (EMG) for bilateral rehabilitation after stroke. Chen et al. [14] proposed a soft exoskeleton glove system (SExoG), which was driven by EMG for bilateral training. However, to the best of our knowledge, almost every existing glove module could only achieve one directional pulling effect. For example, glove modules may have the closing function of hands but cannot simultaneously have the opening function. Therefore, we proposed a bidirectional hand support strategy and integrated it into the bidirectional support glove. The glove used two pairs of bidirectional Bowden cables to stretch in two directions

sequentially, enabling the glove to perform both hand closing and opening functions.

The development of research on exosuits has brought challenges in controlling exosuits. EMG is a biological signal with temporal features, and it is widely used for identifying movement intentions [15] and operating rehabilitation devices to assist treatment [16]. Gesture recognition is one of the most commonly used methods, but hand motor impairments result in neuromuscular pathway changes that affect EMG signal collection [17]. Muscle synergy is a neural control strategy with high robustness [18]. It has become a standard method for extracting coordination patterns from EMG signals and evaluating motor control strategies [19]. Even under the impact of changes in neuromuscular pathways, a reduced set of muscle synergies can reconstruct the original EMG envelopes [20]. The common modulation of the EMG envelope has been shown to reveal synchronized activation of synergistic muscle groups [21], therefore, muscle synergy has been successfully used in rehabilitation [22] and extended to gesture recognition [23]. Moreover, daily tasks require the coordination of both hands using dynamic and static gestures. Dynamic gestures are a series of continuous movement gestures [24], and the related muscles change over time. Human's healthy hands using dynamic and static gestures to coordinate is a natural movement pattern, and bilateral training for degraded hands is a rehabilitation strategy based on natural inter-limb coordination [25]. The coupling movements of both hands can accelerate the reorganization of brain mappings on the affected hemisphere [26] and contribute to the recovery of damaged limbs [27]. However, there are few exosuit studies based on bilateral coordination assistance with dynamic and static gestures. In our study, a bilateral coordination assistance strategy was proposed that recognized the dynamic and static gestures of the healthy hand, driven the bidirectional support glove of the affected hand, and performed corresponding symmetrical and assistive gestures to complete bilateral training tasks [28] and daily tasks.

In recent years, deep learning has been widely used in computer vision [29], image generation [30], and natural language processing [31]. Deep neural networks can extract and learn useful features from raw inputs and classify them in an end-to-end mode. Therefore, deep neural networks are also applied in gesture classification [32]. Convolutional neural network (CNN) is commonly used for gesture recognition. CNN has powerful feature extraction capabilities, but it has a shortcoming against large-scale datasets [33]. Long short-term memory model (LSTM) is an improved network structure based on Recurrent Neural Network (RNN). LSTM has strong advantages in modeling time-series data [34], so it is also used for solving the EMG classification problem. Graph Neural Network (GNN) is an emerging deep learning architecture that operates on graphs, and it has shown excellent performance in capturing feature-based information and modeling complex topological relations [35]. Graph convolutional network (GCN) is an efficient variant of GNN [36], and GCN uses local filters to aggregate information from neighboring nodes [37]. GCN can reflect the muscle synergy by extracting the topological features of EMG signals in the discrete spatial domain [38]. Inspired by the previous studies, we proposed a dynamic gesture recognition model with GCN-LSTM, which combined the advantages of GCN in spatial features and LSTM in temporal features, using spatio-temporal features of EMG to identify movement intentions and classify dynamic and static gestures.

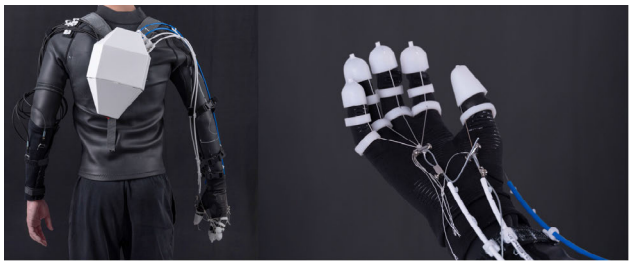

Fig. 1. Overview of the exosuit system and the bidirectional support glove.

In this paper, we proposed an exosuit system with bidirectional hand support for bilateral assistance based on a dynamic gesture recognition model using GCN-LSTM. In the proposed system, the results obtained from the dynamic gesture recognition model were used to drive the bidirectional support glove and provide bilateral coordination assistance of healthy and affected hands. The system included a wearable hardware subsystem and a software subsystem. The wearable hardware subsystem assisted the patient's upper limbs, and the software subsystem recognized the patient's gestures through a dynamic gesture recognition model. An offline training experiment was designed to collect six-channel EMG signals from each subject for training the dynamic gesture recognition model, and two online control experiments were designed to verify and evaluate the effectiveness of the proposed system. The major contribution of this study was the bidirectional hand support strategy, which used a single glove module with bidirectional Bowden cables to push and pull the fingers to perform hand closing and opening movements. Furthermore, a bilateral coordination assistance strategy and a dynamic gesture recognition model were proposed as secondary contributions. The bilateral coordination assistance strategy used the healthy hand to drive the affected hand in performing symmetrical and assistive gestures, and helped patients to complete bilateral training and daily tasks. The dynamic gesture recognition model used GCN-LSTM to collect the spatio-temporal features of multi-channel EMG signals and obtained higher accuracies in dynamic and static gesture classification.

II. Material and Methods

A. System Architecture

The exosuit system includes a hardware subsystem and a software subsystem as shown in Fig. 2. The hardware subsystem includes a double-layer exosuit jacket, a backpack module with integrated hardware, an EMG control module, and a bidirectional support glove. The software subsystem collects the EMG signals from the forearm of the healthy hand, inputs data into the pre-trained dynamic gesture recognition model, classifies the gestures and converts the results into motor control signals to drive the glove of the affected hand.

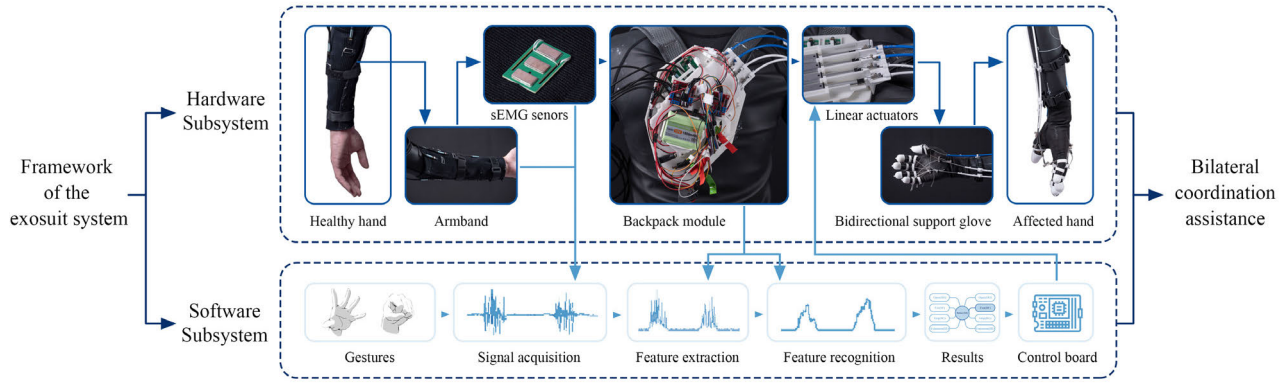

Fig. 2. Framework of the exosuit system.

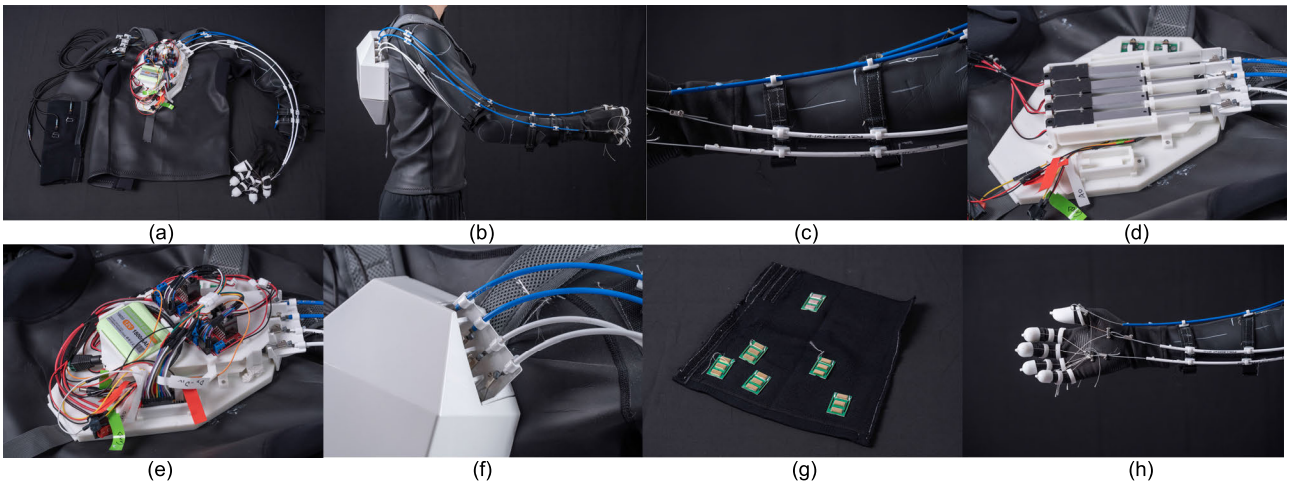

Fig. 3. The hardware subsystem of the exosuit.

B. Hardware Subsystem

1) Exosuit Jacket: The exosuit jacket adopts a double-layer design. The base layer is a neoprene jacket, which provides basic wearing functions. Neoprene is a spongy elastic material, and it provides the necessary compliance and stiffness. The outer layer is stitched with multiple velcro fasteners, which are used to connect to the back strap, anchor points and Bowden cables (Fig. 3a). The ideal routes of the four cables are determined based on lines of non-extension [39] to facilitate the arm's extension and flexion movements (Fig. 3b). Two sizes of anchor points are designed to restrain Bowden cables and EMG signal wires (Fig. 3c).

2) Backpack Module: The backpack module includes a base plate, a case, and a cable limiter, all made by 3D printing. The base plate is equipped with a three-layer modular component. An Arduino Nano control board, six EMG signal processing boards (Wuxi Sichrui Co., Ltd., Wuxi, Jiangsu, China), four micro linear actuators (Xiamen Taihengli Solar Technology Co., Ltd., Xiamen, China) which provide a thrust up to 30N, two actuator driver boards (L298N) and a lithium battery (12V, 3000mA) are installed on the modular component from bottom to top as shown in Fig. 3d, 3e. The case covers all the hardware, and the cable limiter (Fig. 3f) guides the direction of four Bowden cables.

3) EMG Control Module: The EMG control module consists of dry electrode EMG sensors (Wuxi Sichrui Co., Ltd., Wuxi, Jiangsu, China), a fabric armband, and velcro straps, as shown in Fig. 3g. Six sensors are sewed on the armband to collect EMG data from the related muscles of the healthy hand. Velcro straps can keep the sensors close to the skin.

4) Bidirectional Support Glove: The bidirectional support glove consists of a fabric glove base, 3D printed finger modules, and sewing threads with cable fasteners, as shown in Fig. 3h. Each finger module has two holes for passing sewing threads. The sewing threads through the finger modules are connected to the bidirectional Bowden cables by the cable fasteners. The cable fastener is a stainless-steel alloy accessory which can connect two different cables. The fingers can be driven by the bidirectional Bowden cables to perform the opening and closing functions of the hand.

C. Software Subsystem

1) Dynamic Gesture Recognition Framework: The dynamic gesture recognition model with GCN and LSTM consists of a preprocessing layer, a GCN layer, a LSTM layer, and an output layer as shown in Fig. 4. The input of the model are EMG signals, and the output are nine dynamic and static gestures. The GCN layer is used to extract the spatial topological features of EMG, and the LSTM layer is used to extract the temporal features of EMG.

The preprocessing layer is for data processing and constructing graph data. The input is 6-channel EMG signals

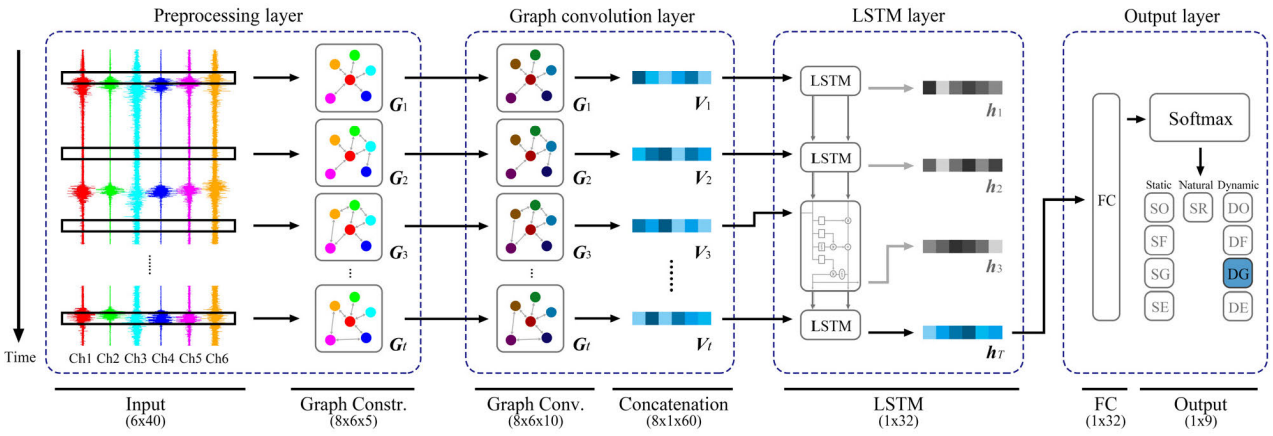

Fig. 4. The diagram of the dynamic gesture recognition framework.

[6 × 40], each EMG channel correspond to a node of the graph data, and the connections between two different nodes correspond to the edges of the graph. An undirected graph to describe the topological structure of the EMG data is defined as $\boldsymbol{G} = (\boldsymbol{V}, \boldsymbol{E})$, where $\boldsymbol{V}$ represents the set of nodes with the number of $|\boldsymbol{V}| = N$ and $\boldsymbol{E}$ represents the set of edges connecting these nodes. By calculating the Euclidean distance between nodes, the relationship between nodes is constructed. The entry of adjacency matrix is denoted by w_{ij} to measure the importance of the connection between the i -th node and the j -th node. As a similarity measure between nodes, Euclidean distance can reflect changes in node relationships in the dynamic process. By applying the Gaussian kernel function, the Euclidean distance between nodes is converted into a similarity score, which makes the dynamic correlation of nodes in the graph data more obvious, thus obtaining dynamic graph data [8×6 × 5]. The Gaussian kernel function can be expressed as

$$w_{ij} = \begin{cases} \exp\left(-\dfrac{\left[dist\,(i,j)\right]^2}{2\theta^2}\right), & if\ dist\,(i,j) \le \tau \\ 0, & otherwise, \end{cases} \tag{1}$$

where θ and τ are two fixed parameters, θ represents the bandwidth of the Gaussian kernel, τrepresents the limit of the Euclidean distance, $dist\,(i, j)$represents the distance between the i -th node and the j -th node. In the graph data structure, it represents the distance similarity between the EMG nodes within the temporal window. Then, the dynamic graph data is spliced in time series to form a dynamic graph data sequence $[\boldsymbol{G}_1, \boldsymbol{G}_2, \ldots, \boldsymbol{G}_T]$, where T represents the window length of the time series graph data.

The obtained dynamic graph data sequence $[\boldsymbol{G}_1, \boldsymbol{G}_2, \ldots, \boldsymbol{G}_T]$ is then input into GCN layer. The graph convolution operation can be expressed in the GCN model as

$$\hat{\boldsymbol{A}} = \boldsymbol{A} + \boldsymbol{I} \tag{2}$$

$$\hat{\boldsymbol{D}}_{ii} = \sum\nolimits_i \hat{\boldsymbol{A}}_{ij}, i = 1, 2, \ldots, N \tag{3}$$

$$\boldsymbol{H}^{l+1} = \sigma\left(\hat{\boldsymbol{D}}^{-1/2}\hat{\boldsymbol{A}}\hat{\boldsymbol{D}}^{-1/2}\boldsymbol{H}^{l}\boldsymbol{W}^{l}\right) \tag{4}$$

where $\hat{\boldsymbol{A}}$ in formula (2) is the adjacency matrix $\boldsymbol{A}$ plus the identity matrix $\boldsymbol{I}$, which represents the relationship matrix of the edge plus the self-loop, $\hat{\boldsymbol{D}}$ in formula (3) is the diagonal matrix of $\hat{\boldsymbol{A}}$, $\boldsymbol{H}^{l}$ and $\boldsymbol{H}^{l+1}$ in formula (4) are the l -th convolution layer and the $l+1$ -th convolution layer, which represent the transfer and update of node features in the graph data to obtain graph data after aggregating spatial features [8×6×10]. The node features obtained in the graph structure are spliced and converted into an one-dimension vector $[V_1, V_2, \ldots, V_T]$ [8×1 × 60], and then input into the LSTM model to extract time information to obtain a spatio-temporal fusion feature.

$$\boldsymbol{I}_t = \sigma\left(\boldsymbol{V}_t\boldsymbol{W}_{vi} + \boldsymbol{h}_{t-1}\boldsymbol{W}_{hi} + \boldsymbol{C}_{t-1}\boldsymbol{W}_{ci} + b_i\right) \tag{5}$$

$$\boldsymbol{F}_t = \sigma\left(\boldsymbol{V}_t\boldsymbol{W}_{vf} + \boldsymbol{h}_{t-1}\boldsymbol{W}_{hf} + \boldsymbol{C}_{t-1}\boldsymbol{W}_{cf} + b_f\right) \tag{6}$$

$$\boldsymbol{C}_t = \boldsymbol{I}_t \tanh\left(\boldsymbol{V}_t\boldsymbol{W}_{vc} + \boldsymbol{h}_{t-1}\boldsymbol{W}_{hc} + b_c\right) + \boldsymbol{F}_t\boldsymbol{C}_{t-1} \tag{7}$$

$$\boldsymbol{O}_t = \sigma\left(\boldsymbol{V}_t\boldsymbol{W}_{vo} + \boldsymbol{h}_{t-1}\boldsymbol{W}_{ho} + \boldsymbol{C}_{t-1}\boldsymbol{W}_{co} + b_o\right) \tag{8}$$

$$\boldsymbol{h}_t = \boldsymbol{O}_t \tanh\left(\boldsymbol{C}_t\right) \tag{9}$$

LSTM saves a long list of historical messages through a memory unit and three control gates. LSTM includes input gate, forget gate, output gate and a cell unit. At time t, the output data of the neuron is $\boldsymbol{h}_t$ [1 × 32].

In the output layer, the 16 original vectors output by the LSTM model are input to the fully connected layer, and 9 vectors suitable for classification are obtained. The results are then output through the softmax layer, representing the possibility of gesture classification for control of the bidirectional support glove. There are nine categories of dynamic and static gesture results.

2) Control Strategy: A bidirectional movement is a pair of bidirectional Bowden cables driven sequentially from opposite directions by two micro linear actuators. The classification results from the dynamic gesture recognition model are upload to the control board, which drives the micro linear actuators to pull or push the bidirectional Bowden cables to perform the target gestures. The thumb's movement is defined as one bidirectional movement and the remaining four fingers' movement is defined as the other bidirectional movement. The same control strategy is applied to both dynamic and static gestures. The Relax gesture is a natural gesture, involving two pairs of Bowden cables are pushed out together to keep all

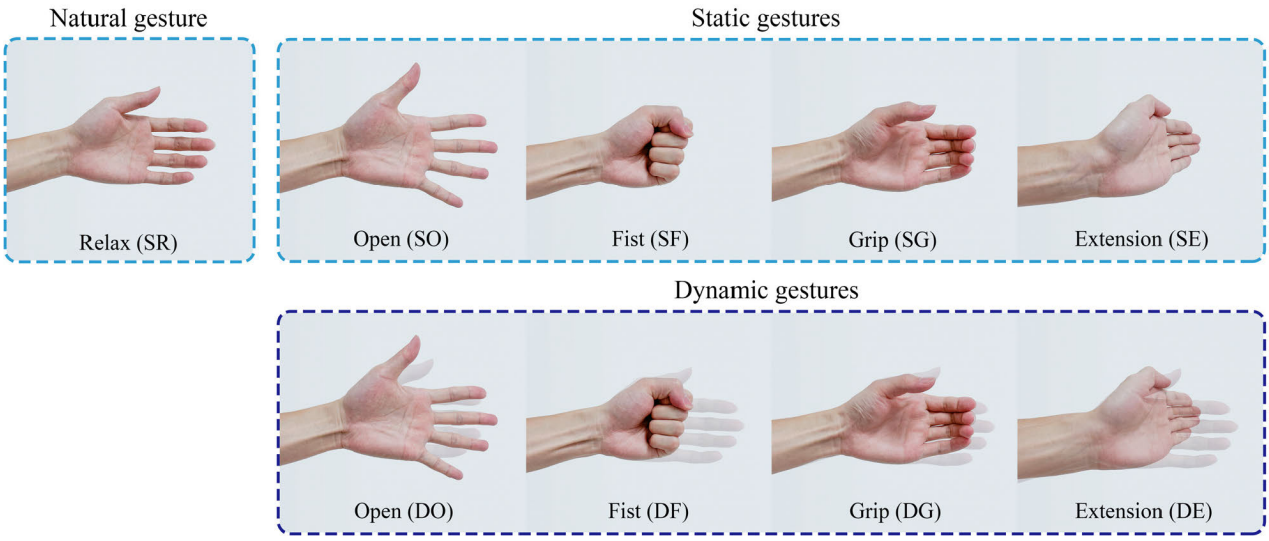

Fig. 5. The dynamic and static gestures related to the tasks: Relax (SR), Open (SO-DO), Fist (SF-DF), Grip (SG-DG), and Extension (SE-DE).

four cables relaxed. The Open and Fist gestures are a pair of symmetrical gestures, involving two pairs of Bowden cables being pulled and pushed out on the same side simultaneously. Similarly, the Grab and Extension gestures are a pair of assistive gestures, involving two pairs of Bowden cables being pulled and pushed out on different sides alternately.

III. Experiments

An offline training experiment and two online control experiments were designed for our exosuit system to verify the accuracies of gesture recognition and performance under different tasks. In the offline training experiment, a dynamic gesture recognition model with GCN-LSTM was constructed for each subject to recognize their gestures. In the online control experiment, the subjects controlled the exosuit system to perform target gestures and completed bilateral coordination tasks, and the results of the tasks were evaluated.

A. Subjects

Sixteen healthy graduate students (8 males and 8 females, ages: 24.8 ± 1.1 years; height: 169.7 ± 7.1 cm; weights: 60.6 ± 8.1 kg) participated in our experiments. All subjects signed informed consent forms before the experiments. All experiments were approved by the Ethics Committee of the Industrial Design Institute, Zhejiang University of Technology (0412/2023/20230012).

B. Offline Training Experiment

The purpose of the offline training experiment was to collect data to construct a gesture recognition model for each subject, and to verify the gesture recognition performance can meet the experimental requirements. Nine commonly used daily life gestures were selected, as shown in Fig. 5. For description, the names of the gestures were encoded into five groups based on dynamic and static gestures: SR for Relax, SO/DO for Open, SF/DF for Fist, SG/DG for Grip and SE/DE for Extension. Relax was defined as the natural gesture in static gesture.

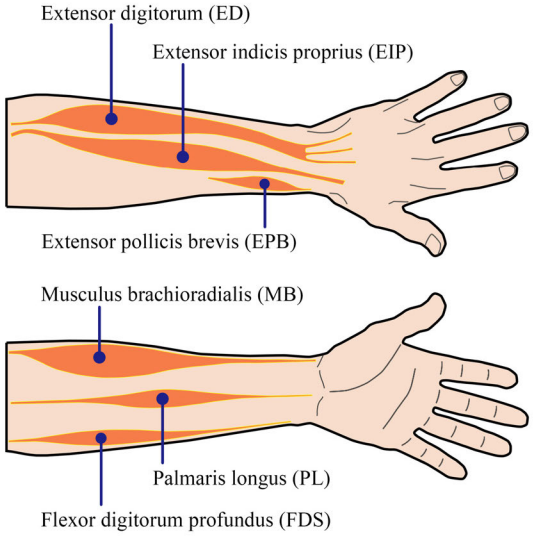

Fig. 6. The related forearm muscles and surface electrode placement locations.

The EMG acquisition equipment was a MP150 (BIOPAC Systems, Inc., USA) and the related muscles in this study include: (1) flexor digitorum profundus (FDS), (2) palmaris longus (PL), (3) musculus brachioradialis (MB), (4) extensor indicis proprius (EIP), (5) extensor digitorum (ED) and (6) extensor pollicis brevis (EPB) as shown in Fig. 6. The subject's forearm skin was cleaned before the experiment, and Ag/AgCl electrodes were attached to the related muscles to obtain EMG signals. Subjects performed the gestures following the visual and verbal instructions given by the experiment host in the order of Relax - Open - Fist - Grip - Extension. For each set of experiment, the specific gesture was performed for 1 second and rest for 4 seconds to avoid fatigue. Each set of gesture was repeated 50 times, with a 5-minute rest between each set. Each gesture was recorded at a sampling frequency of 1 KHz for a total of 250 seconds, obtaining 250,000 samples per gesture.

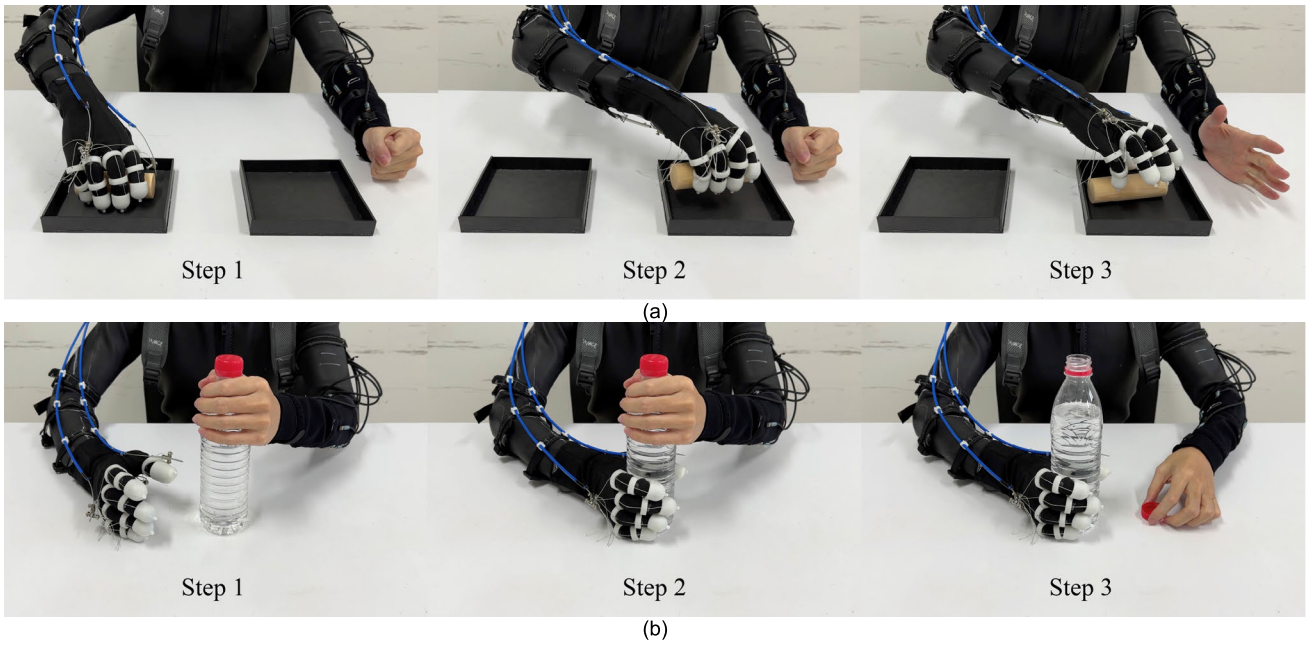

Fig. 7. The two online control sub-experiments.

The obtained EMG data were preprocessed, including filtering, manual slicing, window division, normalization, and label setting. The preprocessing of EMG signals is a fundamental step in extracting valuable information from the raw EMG signals and then use the information as input to the classifier. Matlab 2019b (The MathWorks, Inc., Natick, MA, USA) was used for offline data analysis. A 20-500 Hz bandpass filter and a 50 Hz notch filter were used to remove noise and power frequency interference from the collected EMG data, and the root mean square values (RMS) were used to further process the data. Then, according to the gestures performed in the experiment, manual slicing was used to extract dynamic and static gestures respectively, and then divided the windows. The window length was set to 800ms with a step size of 200ms, with each EMG segment having the same length, moving sequentially from the beginning of the selected sequence to its end. During normalization, the maximum value of the EMG signal obtained in each channel was used as the normalized maximum value. Normalization was applied to the EMG data, defined as follows:

$$x_{\text{nrom}}^{i,j} = \frac{x^{i,j} - x_{\min}^{j}}{x_{\max}^{j} - x_{\min}^{j}} \ldots\ldots \forall i, j \tag{10}$$

70% of the normalized EMG data set was used for training the GCN-LSTM model, and 30% of the data set was used for testing. In addition, to compare with other methods, LSTM [34], CNN [33] and GCN [37] were selected to train gesture recognition models on the same training set respectively, and these models were tested using the same testing set.

C. Online Control Experiments

The purpose of the online control experiments was to evaluate the performance of the exosuit system in bilateral training and bilateral coordination assistance. The experiments were conducted indoor where temperature, humidity, and ventilation conditions were suitable. The experiment host helped the subjects wear the exosuit system and adjust all the modules. The subjects then sat naturally in a chair, and different target objects were placed on the table in front of them.

Firstly, the subjects practiced bilateral training with static symmetrical gestures to become familiar with the control of the exosuit system. The subjects performed a set of static gestures with their healthy hand in the given order, driving the glove module of the affected hand to make symmetrical gestures, and repeated at least five sets. These static symmetrical gestures correspond to bilateral repetitive rehabilitation training.

Next, subjects performed dynamic gestures to complete bilateral tasks. Two daily tasks were selected as two sub-experiments, corresponding to two bilateral coordination assistance functions. Sub-experiment One was to grasp and move the target object, which is a common task in daily life. Two black trays were placed 20cm in front of the subject, and the two trays were 10cm apart. A rigid cylinder was placed in the left tray which close to the affected hand as the target object as shown in Fig. 7a. Firstly, the subject was asked to move the affected hand above the target object and the healthy hand made the Fist gesture; secondly, the subject used the affected hand to grasp the target object and move it to the right tray; finally, the healthy hand made the Open gesture and the affected hand put the target object down. Subjects were required to make 10 grasping attempts on the target object. These dynamic symmetrical gestures correspond to the use of bilateral coordination assistance to complete daily tasks. Sub-experiment Two was to open a bottle cap. Opening a bottle cap is a common task requiring different gestures from both hands to assist, and the gestures need to be highly complementary. A bottle of water (500ml, nearly

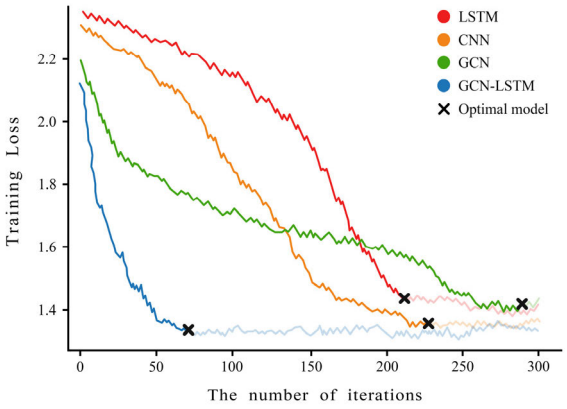

Fig. 8. A representative example of training loss curves of four deep neural network models (LSTM, CNN, GCN and GCN-LSTM) from subject 2.

cylindrical) was placed 20cm in front of the subject as shown in Fig. 7b. Firstly, the subject was asked to grasp the upper part of the bottle with the healthy hand and make the Grip gesture naturally; secondly, the subject moved the affected hand to the lower part of the bottle and performed the corresponding Grip gesture to stabilize the bottle; finally, used the healthy hand to open the bottle cap. Subjects were required to make 10 attempts to open the cap. These dynamic assistive gestures corresponded to the use of bilateral coordination assistance to complete complex daily tasks.

IV. Results

A. Results of Offline Training Experiment

Each subject's data was used to train his own models using four deep neural network classification methods and all subjects obtained models with good convergence results. A representative example of training loss curves of four methods (LSTM, CNN, GCN and GCN-LSTM) from subject 2 are shown in Fig. 8. The horizontal X-axis represents the number of iterations, the vertical Y-axis represents the value of loss, and the black cross represents the model with optimal parameters selected by the early stopping method. The GCN-LSTM model is fitted at 60 epochs, and it converges faster than the other three models. Moreover, at their best parameters, the GCN-LSTM model has a smaller loss value than the other three models, i.e., the proposed model has faster classification speed and better classification performance.

Table I shows the average classification accuracies of all subjects in the four methods. The same subject has different classification accuracies in different models and the same subject can obtain higher classification accuracies in the GCN-LSTM model. The remaining three methods, i.e., LSTM, CNN, and GCN, were also used to train the recognition models with the same training set for each subject to compare with the proposed method. The average confusion matrices of four methods for testing set across all subjects are shown in Fig. 9. The vertical axis of the matrix represents the actual category of the test data set, the horizontal axis represents the corresponding predicted category. The main diagonal entries represent the average percentages of correct classification samples, and the off-diagonal entries represent the average percentages of misclassification samples. According to Fig. 9, the GCN-LSTM model achieves good performance in all nine dynamic and static gesture accuracies. In the proposed method, the SR achieves the highest accuracy at 100% and the SG achieves the lowest accuracy at 88%. The other three methods performed well in the recognition of static gestures, while all performed poorly in the recognition of dynamic gestures.

TABLE I
The Results of Average Classification Accuracies for Each Subject

Subjects	LSTM (%)	CNN (%)	GCN (%)	GCN-LSTM (%)
1	87.77	87.28	85.86	98.40
2	85.44	86.75	82.49	97.42
3	91.41	92.03	81.87	96.99
4	92.32	91.91	83.35	97.10
5	90.30	91.58	84.87	97.82
6	88.11	92.49	75.13	97.82
7	87.04	89.70	83.86	98.65
8	90.86	92.27	76.30	98.65
9	75.92	77.43	83.91	93.87
10	70.81	74.37	75.65	92.15
11	72.16	80.59	83.77	93.67
12	84.32	78.08	78.65	96.22
13	77.56	77.60	77.51	94.59
14	77.11	81.46	85.30	95.88
15	82.31	83.97	78.52	96.91
16	83.85	85.79	85.48	97.20
Average	83.58	85.21	81.41	96.42
± std	± 6.94	± 6.25	± 3.80	± 1.92

TABLE II
The Results of Average Success Rate and Task Execution Time for Each Subject in the Sub-Experiment One

Subjects	Success Rate (%)	Execution Time (s)	Relax (%)	Fist (%)	Open (%)
1	100	18.07	96.72	90.30	94.46
2	100	19.39	96.59	93.58	92.99
3	80	17.93	93.10	90.30	92.95
4	80	20.25	89.58	88.81	87.42
5	80	19.74	89.48	86.51	85.55
6	100	19.18	90.58	89.31	86.58
7	70	20.65	94.29	91.50	88.95
8	90	18.55	93.83	90.76	89.11
9	100	18.99	93.93	91.03	88.83
10	70	20.61	99.15	77.76	92.17
11	100	19.32	99.19	75.69	92.90
12	100	18.60	97.67	74.90	91.18
13	90	19.13	97.79	75.94	90.43
14	80	18.63	97.07	74.86	92.55
15	90	17.86	96.45	76.56	88.46
16	90	18.52	97.14	76.90	88.19
Average	88.75	19.09	95.16	84.04	90.17
± std	± 10.88	± 0.88	± 3.18	± 7.42	± 2.65

B. Results of Online Control Experiments

In the online control experiments, the results of the two bilateral coordination assistance sub-experiments are shown in Table II and Table III. The results are composed of average bilateral control success rates, average task execution time and related gesture recognition rates. The average bilateral control success rate is defined as the percentage of the number

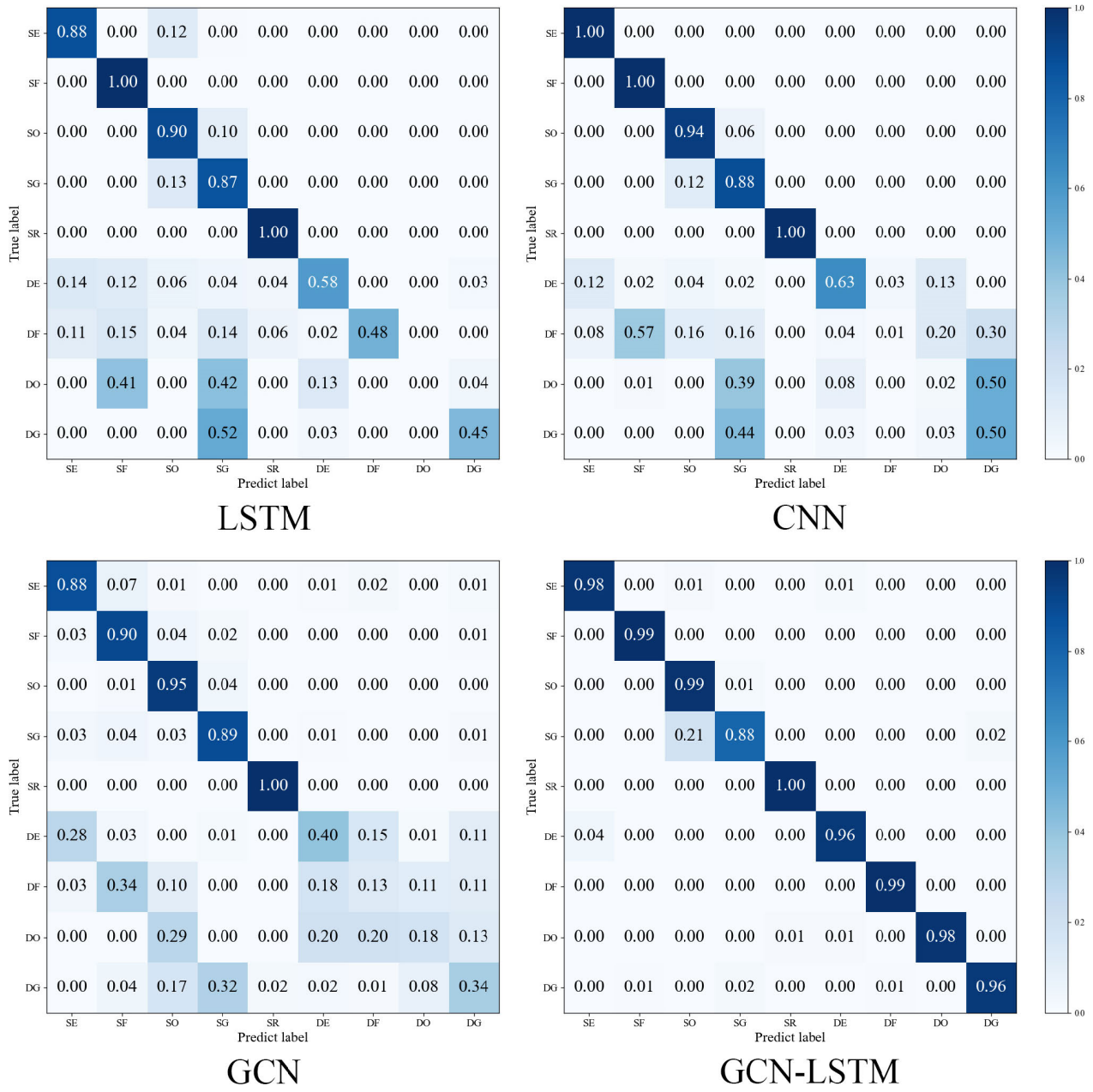

Fig. 9. The average confusion matrices of four methods for testing set across all subjects.

of times that the subject completed the task. The average task execution time refers to the time taken by a subject to complete the daily bilateral task, starting from the Relax gesture and proceeding through a series of target gestures. The related gesture recognition rates represent the relevant gestures involved in the tasks and their gesture recognition rates.

In Sub-experiment One, for all subjects, the average bilateral control success rate is 88.75% and the average task execution time is 19.09 seconds. The subject with the best performance was able to control the exosuit system to grasp, lift the object, and move it to the target place within 17.93 seconds. The involved gesture recognition rates are 95.16% (Relax), 84.04% (Fist) and 90.17% (Open). In Sub-experiment Two, for all subjects, the average bilateral control success rate is 86.88% and the average task execution time is 17.47 seconds. The subject with the best performance was able to control the exosuit system to stabilize the water bottle and open the bottle cap within 16.28 seconds. The related gesture recognition rates are 95.51% (Relax), 84.99% (Grip) and 89.38% (Open).

V. Discussion

The offline training experiment and the online control experiments both showed suitable results, and fully verified the effectiveness of the proposed exosuit system.

The results of the offline training experiment showed that the proposed GCN-LSTM model achieved higher average dynamic gesture recognition rate (96.42%) than LSTM, CNN and GCN models. One reason is that GCN model has

TABLE III
THE RESULTS OF AVERAGE SUCCESS RATE AND TASK EXECUTION TIME FOR EACH SUBJECT IN THE SUB-EXPERIMENT TWO

Subjects	Success Rate (%)	Execution Time (s)	Relax (%)	Grip (%)	Open (%)
1	100	16.29	95.41	84.32	92.93
2	90	17.14	96.48	84.32	92.57
3	90	17.52	96.21	83.55	92.27
4	70	16.76	90.29	89.08	85.43
5	100	17.47	92.96	87.36	85.72
6	90	17.77	92.93	87.80	85.99
7	90	17.61	94.81	95.17	88.26
8	80	18.28	94.72	95.38	88.12
9	100	18.66	94.68	94.88	88.29
10	70	17.41	98.51	87.23	93.06
11	100	17.95	98.63	86.54	93.42
12	70	17.74	96.98	76.97	89.55
13	100	17.25	97.44	76.01	89.53
14	80	17.41	95.99	79.25	89.76
15	90	16.65	95.78	74.94	86.49
16	70	17.61	96.27	76.97	88.75
Average	86.88	17.47	95.51	84.99	89.38
± std	± 11.95	± 0.59	± 2.15	± 6.80	± 2.76

advantages at processing non-Euclidean structured data by extracting the deep features and topological features of graph data. GCN obtains and integrates the spatial topological features of 6-channel EMG signals from different muscles, and the pattern of muscle synergy is consistent with spatial topological features of the EMG signals. Lee et al. [38] used a stretchable array sensor to acquire EMG activities of 18 different gestures and recognized dynamic and static gestures with an accuracy of 97% by a self-attention-based graph neural network. The other reason is that LSTM model has advantages at extracting temporal features from EMG signals, and dynamic gestures are consistent with temporal changes. Wu et al. [40] took advantages of the complementarity of LSTM and CNN by combining them into one architecture (LCNN). They achieved an average accuracy of 98.14% for dynamic gestures by using LSTM to extract temporal information and CNN to extract secondary features. Compared with the other three traditional methods, the proposed method achieves better dynamic gesture recognition rate because it obtains the spatial topological features and temporal features of 6-channel EMG simultaneously. In addition, the other three traditional methods all achieve high recognition rates for static gestures and low recognition rates for dynamic gestures. One reason is that the corresponding dynamic and static gesture movements has high similarity, which increases the possibility of misrecognition. Another reason is that the amount of static gesture data is larger than dynamic gesture data in the same data set. For example, the Relax gesture presents in all nine gestures, resulting in the largest amount of data and thus achieving the highest recognition rate in each method.

The results of the online control experiments showed that the proposed exosuit system achieved high bilateral coordination success rates and short task execution times, indicating high stability and timely response speed in daily tasks. Additionally, the system can accurately recognize and execute gestures and successfully return to the default Relax gesture after task completion. One reason is that the proposed model has outstanding classification performance (96.42%), which results in a decent task success rate. The other reason is that the proposed exosuit system was designed with meticulous consideration. The lengths and routes of the bidirectional Bowden cables were precisely measured. By referring to the lines of non-extension [39], the bidirectional Bowden cables were ensured to be pushed and pulled in the shortest path, so that the fingertips could obtain the highest force transmission efficiency [41]. Therefore, when the linear actuators are fully pushed out, the length of the cable allows the affected hand to relax, and when the linear actuators are fully pulled back, the length of the cable counteracts the elbow extension and the maximum pulling force can be transmitted to the fingertips, allowing the glove module to achieve better gripping performance. However, misclassifications still occurred in the sub-experiments. The reason is that the proposed model did not achieve a completely accurate recognition rate and the subjects were unable to maintain the same gesture during multiple gesture movements.

In addition, all 16 subjects who completed the online control experiments agreed or strongly agreed that the proposed exosuit system would be useful in assisting daily tasks. Many subjects reported feeling strong force feedback from the bidirectional support glove during the tasks. The bidirectional hand support strategy and the bilateral coordination assistance strategy can also be applied to the design of exosuits for other limbs, such as bidirectional elbow support or bilateral assistance for lower limbs, which can provide new thoughts for exosuit design and research in the future.

One limitation of this study is that, although we compared representative models based on EMG, some new models and new methods (i.e., computer vision and sensors) are still worth studying. In future studies, we will continue to explore and compare these models and methods to verify the effectiveness of our proposed strategies and model.

VI. CONCLUSION

In this paper, we proposed an exosuit system with bidirectional hand support for bilateral coordination assistance based on dynamic and static gesture recognition model with GCN-LSTM, including a hardware subsystem and a software subsystem. The proposed hardware subsystem enabled patients to use their healthy hand to drive the affected hand, allowing them to perform symmetrical and assistive gestures to complete daily tasks and enhance their life abilities. The proposed software subsystem combined the advantages of GCN and LSTM into a dynamic gesture recognition model, which makes up for the shortcoming of the exosuit system without dynamic gesture control. The experimental results showed that the proposed method improved the recognition rate of dynamic and static gestures to 96.42% ± 3.26%, compared to three traditional classification models. The designed exosuit hardware and software subsystems can perform the target gestures successfully and complete daily tasks bilaterally. The proposed system can improve the patient's self-care and rehabilitative ability effectively by natural human-computer interaction. In addition, our study can provide new methods

for the design of exosuit systems and application of bilateral assistance.

REFERENCES

[1] Y. Wang, S. Cang, and H. Yu, "A survey on wearable sensor modality centred human activity recognition in health care," *Exp. Syst. Appl.*, vol. 137, pp. 167–190, Dec. 2019.

[2] P. Polygerinos, K. C. Galloway, S. Sanan, M. Herman, and C. J. Walsh, "EMG controlled soft robotic glove for assistance during activities of daily living," in *Proc. IEEE Int. Conf. Rehabil. Robot. (ICORR)*, Singapore, Aug. 2015, pp. 55–60.

[3] A. Cisnal, J. Pérez-Turiel, J.-C. Fraile, D. Sierra, and E. de la Fuente, "RobHand: A hand exoskeleton with real-time EMG-driven embedded control. Quantifying hand gesture recognition delays for bilateral rehabilitation," *IEEE Access*, vol. 9, pp. 137809–137823, 2021.

[4] E. M. Frick and J. L. Alberts, "Combined use of repetitive task practice and an assistive robotic device in a patient with subacute stroke," *Phys. Therapy*, vol. 86, no. 10, pp. 1378–1386, Oct. 2006.

[5] V. Longatelli et al., "User-centred assistive SystEm for arm functions in neUromuscuLar subjects (USEFUL): A randomized controlled study," *J. NeuroEng. Rehabil.*, vol. 18, no. 1, p. 4, Dec. 2021.

[6] C. Ochieze, S. Zare, and Y. Sun, "Wearable upper limb robotics for pervasive health: A review," *Prog. Biomed. Eng.*, vol. 5, no. 3, Jul. 2023, Art. no. 032003.

[7] A. S. Gorgey, "Robotic exoskeletons: The current pros and cons," *World J. Orthopedics*, vol. 9, no. 9, pp. 112–119, Sep. 2018.

[8] E. Bardi, M. Gandolla, F. Braghin, F. Resta, A. L. G. Pedrocchi, and E. Ambrosini, "Upper limb soft robotic wearable devices: A systematic review," *J. NeuroEng. Rehabil.*, vol. 19, no. 1, p. 87, Aug. 2022.

[9] A. T. Asbeck, S. M. M. De Rossi, I. Galiana, Y. Ding, and C. J. Walsh, "Stronger, smarter, softer: Next-generation wearable robots," *IEEE Robot. Autom. Mag.*, vol. 21, no. 4, pp. 22–33, Dec. 2014.

[10] S. Lessard, P. Pansodtee, A. Robbins, J. M. Trombadore, S. Kurniawan, and M. Teodorescu, "A soft exosuit for flexible upper-extremity rehabilitation," *IEEE Trans. Neural Syst. Rehabil. Eng.*, vol. 26, no. 8, pp. 1604–1617, Aug. 2018.

[11] T. Abe et al., "Fabrication of '18 weave' muscles and their application to soft power support suit for upper limbs using thin McKibben muscle," *IEEE Robot. Autom. Lett.*, vol. 4, no. 3, pp. 2532–2538, Jul. 2019.

[12] B. Noronha et al., "Soft, lightweight wearable robots to support the upper limb in activities of daily living: A feasibility study on chronic stroke patients," *IEEE Trans. Neural Syst. Rehabil. Eng.*, vol. 30, pp. 1401–1411, 2022.

[13] D. Leonardis et al., "An EMG-controlled robotic hand exoskeleton for bilateral rehabilitation," *IEEE Trans. Haptics*, vol. 8, no. 2, pp. 140–151, Apr. 2015.

[14] Y. Chen, Z. Yang, and Y. Wen, "A soft exoskeleton glove for hand bilateral training via surface EMG," *Sensors*, vol. 21, no. 2, p. 578, Jan. 2021.

[15] K. Y. Ang, Y. Y. Huang, and K. H. Low, "Electromyography analysis for pre-clinical trials of hand rehabilitation tasks using design of experiments," in *Proc. Int. Conf. Mechatronics Autom.*, Changchun, China, Aug. 2009, pp. 915–920.

[16] E. J. Rechy-Ramirez and H. Hu, "Bio-signal based control in assistive robots: A survey," *Digit. Commun. Netw.*, vol. 1, no. 2, pp. 85–101, Apr. 2015.

[17] H. Yang, J. Wan, Y. Jin, X. Yu, and Y. Fang, "EEG- and EMG-driven poststroke rehabilitation: A review," *IEEE Sensors J.*, vol. 22, no. 24, pp. 23649–23660, Dec. 2022.

[18] L. Tang, F. Li, S. Cao, X. Zhang, D. Wu, and X. Chen, "Muscle synergy analysis in children with cerebral palsy," *J. Neural Eng.*, vol. 12, no. 4, Aug. 2015, Art. no. 046017.

[19] G. Torres-Oviedo and L. H. Ting, "Muscle synergies characterizing human postural responses," *J. Neurophysiol.*, vol. 98, no. 4, pp. 2144–2156, Oct. 2007.

[20] A. Scano, L. Dardari, F. Molteni, H. Giberti, L. M. Tosatti, and A. d'Avella, "A comprehensive spatial mapping of muscle synergies in highly variable upper-limb movements of healthy subjects," *Frontiers Physiol.*, vol. 10, p. 1231, Sep. 2019.

[21] T. Liang, H. Miao, H. Wang, X. Liu, and X. Liu, "Surface electromyography-based analysis of the lower limb muscle network and muscle synergies at various gait speeds," *IEEE Trans. Neural Syst. Rehabil. Eng.*, vol. 31, pp. 1230–1237, 2023.

[22] K. Zhao et al., "Muscle synergies for evaluating upper limb in clinical applications: A systematic review," *Heliyon*, vol. 9, no. 5, May 2023, Art. no. e16202.

[23] X. Luo et al., "Synergistic myoelectrical activities of forearm muscles improving robust recognition of multi-fingered gestures," *Sensors*, vol. 19, no. 3, p. 610, Feb. 2019.

[24] Z. Yang et al., "Dynamic gesture recognition using surface EMG signals based on multi-stream residual network," *Frontiers Bioeng. Biotechnol.*, vol. 9, Oct. 2021, Art. no. 779353.

[25] S. M. Waller, M. Harris-Love, W. Liu, and J. Whitall, "Temporal coordination of the arms during bilateral simultaneous and sequential movements in patients with chronic hemiparesis," *Exp. Brain Res.*, vol. 168, no. 3, pp. 450–454, Jan. 2006.

[26] A. R. Luft et al., "Repetitive bilateral arm training and motor cortex activation in chronic stroke: A randomized controlled trial," *Jama*, vol. 292, no. 15, pp. 1853–1861, Oct. 2004.

[27] G. Kwakkel, B. J. Kollen, and H. I. Krebs, "Effects of robot-assisted therapy on upper limb recovery after stroke: A systematic review," *Neurorehabilitation Neural Repair*, vol. 22, no. 2, pp. 111–121, Mar. 2008.

[28] M. E. Stoykov and D. M. Corcos, "A review of bilateral training for upper extremity hemiparesis," *Occupational Therapy Int.*, vol. 16, nos. 3–4, pp. 190–203, Sep. 2009.

[29] X. Li et al., "Transformer-based visual segmentation: A survey," 2023, *arXiv:2304.09854*.

[30] B. Xiao, H. Wu, and X. Bi, "DTMNet: A discrete Tchebichef moments-based deep neural network for multi-focus image fusion," in *Proc. IEEE/CVF Int. Conf. Comput. Vis. (ICCV)*, Montreal, QC, Canada, Oct. 2021, pp. 43–51.

[31] M. R. Kounte, P. K. Tripathy, P. Pramod, and H. Bajpai, "Analysis of intelligent machines using deep learning and natural language processing," in *Proc. 4th Int. Conf. Trends Electron. Informat. (ICOEI)*, Tirunelveli, India, Jun. 2020, pp. 956–960.

[32] U. Cŏté-Allard et al., "Deep learning for electromyographic hand gesture signal classification using transfer learning," *IEEE Trans. Neural Syst. Rehabil. Eng.*, vol. 27, no. 4, pp. 760–771, Apr. 2019.

[33] Y. Liu, X. Li, L. Yang, G. Bian, and H. Yu, "A CNN-transformer hybrid recognition approach for sEMG-based dynamic gesture prediction," *IEEE Trans. Instrum. Meas.*, vol. 72, pp. 1–16, 2023.

[34] C.-F. Chen, Z.-J. Du, L. He, Y.-J. Shi, J.-Q. Wang, and W. Dong, "A novel gait pattern recognition method based on LSTM-CNN for lower limb exoskeleton," *J. Bionic Eng.*, vol. 18, no. 5, pp. 1059–1072, Sep. 2021.

[35] J. Zhou et al., "Graph neural networks: A review of methods and applications," *AI Open*, vol. 1, pp. 57–81, Jan. 2020.

[36] T. N. Kipf and M. Welling, "Semi-supervised classification with graph convolutional networks," 2017, *arXiv:1609.02907*.

[37] T. Danel et al., "Spatial graph convolutional networks," 2019, *arXiv:1909.05310*.

[38] H. Lee et al., "Stretchable array electromyography sensor with graph neural network for static and dynamic gestures recognition system," *Npj Flexible Electron.*, vol. 7, no. 1, p. 20, Apr. 2023.

[39] T. Binedell, U. Gupta, B. Sithanathan, K. Subburaj, and L. Blessing, "Mapping lines of non-extension in persons with lower limb amputation to aid comfort-driven prosthetic socket design," *Med. Eng. Phys.*, vol. 118, Aug. 2023, Art. no. 104018.

[40] Y. Wu, B. Zheng, and Y. Zhao, "Dynamic gesture recognition based on LSTM-CNN," in *Proc. Chin. Autom. Congr. (CAC)*, Nov. 2018, pp. 2446–2450.

[41] D. Chen, Y. Yun, and A. D. Deshpande, "Experimental characterization of bowden cable friction," in *Proc. IEEE Int. Conf. Robot. Autom. (ICRA)*, Hong Kong, May 2014, pp. 5927–5933.